Synthesis, Crystal Structures, Hydrogen Bonds and Antibacterial Activity of New Quinoline Derivatives

Tarek Djemel, Amel Messai, Dominique Luneau & Earwann Jeanneau

Journal of Chemical Crystallography

ISSN 1074-1542

J Chem Crystallogr
DOI 10.1007/s10870-015-0595-x

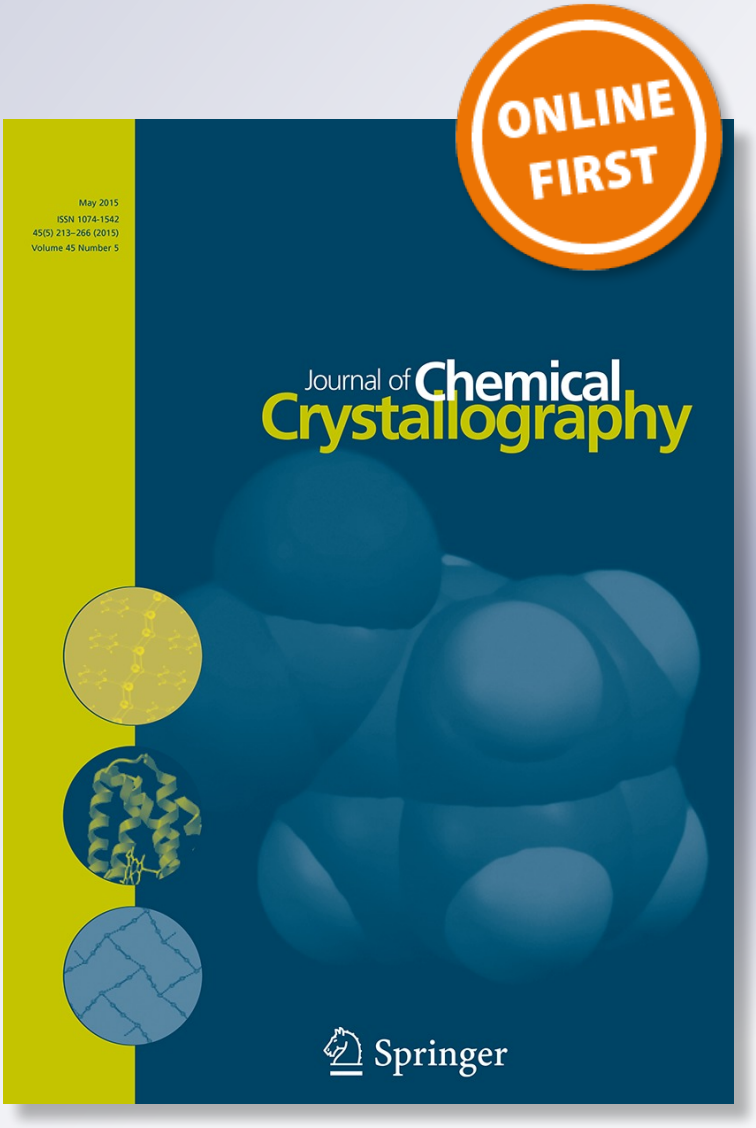

Springer

J Chem Crystallogr
DOI 10.1007/s10870-015-0595-x

ORIGINAL PAPER

Synthesis, Crystal Structures, Hydrogen Bonds and Antibacterial Activity of New Quinoline Derivatives

Tarek Djemel[1] · Amel Messai[1] · Dominique Luneau[2] · Earwann Jeanneau[2]

Received: 31 January 2015 / Accepted: 3 June 2015

Abstract Two new quinolines derivatives where crystallized from the acetylation reaction in low temperature ; between Baylis–Hillman products which had themselves been prepared from the Meth Cohn method and catalyzed by 1,4-diazabicyclo (Fatiha et al. in J Chem Crystallogr 42:989–996, 2012) octane and silicon dioxide or in pyridine and chloroform. Chemical structures have been established by spectral techniques of FTIR, 1H NMR and X-ray single crystal in low temperature. The crystal structure of (**1a**) crystallizes in triclinic space group *P*-1, $a = 7.9145(12)$ Å, $b = 9.1412(11)$ Å, $c = 10.7286(16)$ Å, $\alpha = 94.760(11)°$, $\beta = 105.988(13)°$, $\gamma = 101.818(11)°$, while (**2a**) crystallizes in orthorhombic non- centrosymmetric space group *Pna21*, $a = 7.7237(12)$ Å, $b = 20.2539(28)$ Å, $c = 8.7164(12)$ Å, and its cohesion was found to be assured by O–H···O and C–H···O hydrogen bonds. Antimicrobial activity (in vitro) was evaluated by Gram-positive and Gram-negative bacteria. The compounds have shown good biological activity with Gram-positive bacteria (*Staphylococcus aurous* and *Staphylococcus* coagulase-negative).

Graphical Abstract Two new Quinoline derivatives have been prepared with good products yields; these products constitute original compounds, of great interest biological activity.

✉ Amel Messai
messai.amel@yahoo.ca

[1] Laboratoire des Structures, Propriétés et Interactions Inter Atomiques (LASPI2A), Institut des Sciences et Technologie, Université Abbés Laghrour, 40000 Khenchela, Algeria

[2] Laboratoire des Multimatériaux et Interfaces (UMR 5615), Université Claude Bernard Lyon 1, 69622 Villeurbanne Cedex, France

Published online: 11 June 2015

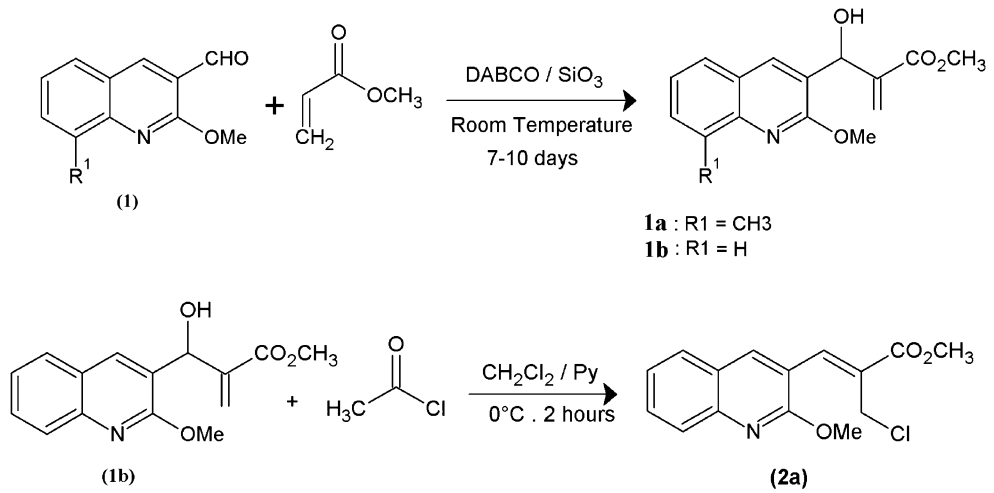

Keywords Quinoline derivatives · Baylis–Hillman reaction · Crystal structure · X-ray diffraction · Hydrogen bond · Antimicrobial

Introduction

The quinoline ring system is a common structural component of a wide variety of natural or synthetically prepared products with highly desirable biological activity [1]. It is a heterocyclic scaffold of paramount importance to human race. Indeed, quinoline derivatives are some of the oldest compounds which have been utilized for the treatment of a variety of diseases [2].

The bark of Cinchona plant containing quinine was utilized to treat palpitations [3] fevers and tertians since more than 200 years ago. Quinoline, a diastereoisomer of quinine was in the early twentieth century acknowledged as the most potent of the antiarrhythmic compounds isolated from the Cinchona plant [4].

Compounds containing quinoline motif are most widely used as antimalarials [5, 6], antifungals [7], antibacterials [8, 9], and antitumor agents [10, 11]. They have antiseptic, antipyretic and antiperiodic properties [12]. Substituted quinolines play also an important role as receptor antagonists of endothelin [13], 5HT3 [14] and NK-3 [15].

Additionally, quinoline derivatives find use in the synthesis of biocides, fungicides, and flavoring agents [16]. These compounds find applications in chemistry of transition-metal catalyst for uniform polymerization and luminescence chemistry [17]. Owing to such as significance, the synthesis of substituted quinolines has been a subject of great focus in organic chemistry.

This paper aims to describe the synthesis, structure and the biological effect of quinolines adducts obtained from the Baylis–Hillman derivates [18]. Those adducts are the result of the acetylation reaction of Baylis–Hillman products in low temperature catalyzed by 1,4-diazabicyclo [2] octane (DABCO) and silicium oxid (**1a**–**1b**) or in pyridine and chloroform (**2a**).

Experimental

Synthesis of Quinoline Derivatives

General Procedure

Baylis–Hillman adducts (**1a**–**1b**) were obtained from the reaction of 2-methoxy-3-formyl quinoline derivatives (1), previously obtained from the Meth Cohn procedure. [19], and methyl acrylate catalyzed by DABCO (Fig. 1) and

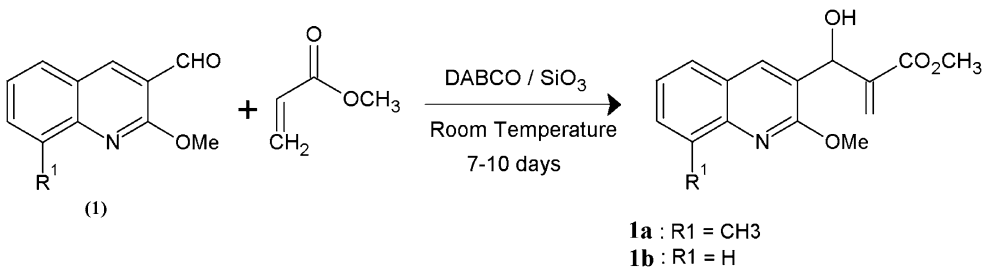

Fig. 1 Synthesis reaction of the compounds **1a**–**1b**

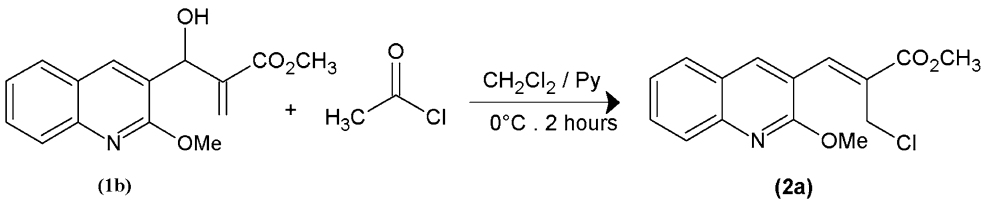

Fig. 2 Synthesis reaction of the compounds **2a**

silicon oxide like solid support at room temperature. These compounds were obtained according to the literature methods published in the paper of Narender et al. [20].

Acetylation of the Baylis–Hillman adduct is generally described as a simple reaction between OH and acetyl chloride in an anhydrous medium. In this case mentioned adducts are acetylated by acetyl chloride in pyridine. Reaction was carried our under the action of acetyl chloride in dichloromethane, pyridine at a temperature of 0 °C; after disappearance of the starting material. We have separated the product (**2a**) as shown in (Fig. 2).

*Synthesis of Methyl 2-[hydroxy(2-methoxy-8-methylquinolin-3-yl)methyl]prop-2-enoate (**1a**)*

The condensation of 2-methoxy-8-methylquinoline-3-carbaldehyde (1.48 mmol) pre- synthesized according to the Meth Cohn method [20], and methyl acrylate (12 ml) catalyses by DABCO and silicon dioxide like solid support at room temperature, allowed to continue for 1 week. Has yielded white powder of (**1a**) (0.42 g; 96 %; m.p = 68 °C. Rf = 0.52 (ethyl acetate/petroleum ether (4/6) which have been recrystallized from chloroform, ethyl acetate and petroleum ether; colorless single crystals were obtains after some days. I.R (KBr; δ cm^{-1}): 3376 (OH), 1734 (COO), 1625 (C=C). ^{1}HNMR ($CDCl_3$, d ppm, 300 MHz), 1.1 (s, 3 H, CH_3), 1.4 (d, J = 6.3 Hz, H, OH), 3.84(s,3H, CO–O–CH_3), 4.4(s, 3H, O–CH_3) 5.79 (d, 1H, J = 1.2 Hz, = CH_2, Ha); 5.89 (d, 1H, J = 5.8 Hz, CHOH), 6.36 (d, 1H, J = 0.9 Hz, Hb, = CH_2, Hb), 7.24–7.74 (m, 4H, ArH),

*Synthesis of Methyl (2Z)-2-(chloromethyl)-3-(2-methoxyquinolin-3-yl)prop-2-enoate (**2a**)*

To a stirred solution of methyl 2-[hydroxy(2-methoxyquinolin-3-yl)methyl]prop-2-enoate (**1b**) (Fig. 1) (0.6 g; 2.2 mmol), wich has themselves been prepared from 2-méthoxy-3-formylquinoléine and methyl acrylate from a general process [19, 20] in pyridine and chloroform at low temperature (0 °C) was added 0.3804 ml (2.44 eq) of acetylchloride. The reaction was allowed to continue for 2 h, the product was crystallized in acetyl acetate, colorless single crystals were obtains in 40 % yied (0.48 g; m.p = 106 °C). Rf = 0.56 (ethyl acetate/petroleum ether (4/6), I.R (KBr; δ cm^{-1}): 1714 (CO), 1601 (C=C), 774 (CH_2Cl). ^{1}HNMR ($CDCl_3$, d ppm, 300 MHz), 2.5 (s, 3 H, CO–OCH_3), 3.7 (s, 3 H, O–CH_3), 4.0 (s, 2 H, CH_2–Cl), 5.2 (s, 1H, CH), 6.3 (s, 1 H, ArH), 7.2 (s, 1H, ArH) 7.4 (s, 1 H, ArH) 7.5 (s, 1 H,ArH) 8.0 (s, 1 H, ArH).

Spectroscopic Measurements

Infrared Analysis

The FTIR has been carried out to analyse the chemical bonding and molecular structure of the compound. The FTIR spectrums of the compounds were recorded in frequency region from 400 to 4000 cm^{-1} with a FTIR NEXUS NICOLET Spectrometer in KBr pellets.

^{1}H NMR and ^{13}C NMR Analysis

The ^{1}H NMR was recorded on a Bruker 300 MHZ instrument at 23 °C to confirm the molecular structure.

X-ray Structure Analysis

Diffraction Data Collection

The structures of (**1a**–**2a**) have been determined by single-crystal X-ray diffraction analysis. X-ray diffraction intensities were collected at 150 K using an Oxford Diffraction Xcalibur, Atlas, Gemini ultra diffractometer with Mo Kα radiation (λ = 0.71073 Å), equipped with the required cooling. The data collection strategy is summarized in (Table 1).

Data Reduction

The unit cell determination and data reduction were performed using the CrysAlis program [21] on the full set of data.

Solution and Refinement

Calculations were carried out using the WinGX software package [22]. The crystal structure was solved by direct methods using SIR2004 [23] and refined by full-matrix least-squares against F^2 using all data (SHELX97) [24].

All non-H atoms were modelled with anisotropic displacement parameters. The H atoms attached to –CH3 and

Table 1 Experimental details of the data collection for (**1a**) and (**2a**)

1a	**2a**
Xcalibur, Atlas, Gemini ultra	Xcalibur, Atlas, Gemini ultra
Diffractometer	Diffractometer
Radiation source: Enhance (Mo) X-ray Source	Radiation source: Enhance (Mo) X-ray source
Graphite monochromator	Graphite monochromator
Detector resolution: 10.4685 pixels mm^{-1}	Detector resolution: 10.4685 pixels mm^{-1}
ω scans	ω scans
Absorption correction: analytical	Absorption correction: analytical
Tmin = 0.976, Tmax = 0.988	Tmin = 0.972, Tmax = 0.972
7760 measured reflections	11,544 measured reflections
3421 independent reflections	3296 independent reflections
2706 reflections with $I > 2\sigma(I)$	2708 reflections with $I > 2\sigma(I)$
$R_{int} = 0.037$	$R_{int} = 0.051$
	Flack x = −0.03(11)
θmax = 29.4°, θmin = 3.9°	θmax = 29.6°, θmin = 3.7°
$h = -10 \rightarrow 10$	$h = -9 \rightarrow 10$
$k = -12 \rightarrow 12$	$k = -23 \rightarrow 27$
$l = -13 \rightarrow 14$	$l = -10 \rightarrow 11$

–OH were located in difference Fourier maps refined as riding atoms (isotropically with a restrained bond distance) with distances constraints of methyl C–H = 0.96 Å and O–H = 0.82 Å [Uiso(H) = 1.5 Ueq(C,O)]. Aromatic H atoms were positioned geometrically and were allowed to ride on their parent C atoms with C–H = 0.93 Å and and Uiso(H) = 1.2Ueq(C).

Crystal structure was visualized using ORTEP3 [25] and MERCURY [26]. Analyses were carried out using the program PLATON [27], as incorporated in the WinGX [22].

Biological Activity

A filter paper sterilized disc saturated with measured quantity of the sample (10 µl, 4–1 mg/ml) is placed on plate containing solid bacterial medium (nutrient agar broth) which has been heavily seeded with spore suspension of the tested organism. The assay plates which incubated at 37 °C for 1 day for bacteria. After inoccupation, the diameter of the clear zone of inhibition surrounding the sample is taken as a measure of the inhibitory power of the sample against the particular test organism [28, 29]. The organisms used included two Gram-positive (*Staphylococcus aurous*; *Staphylococcus* coagulase-negative), and two Gram-negative (*Escherichia coli*; *Pseudomonas aeruginosa*) bacteria.

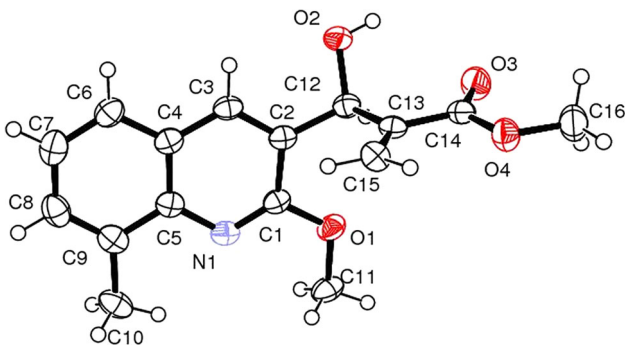

Fig. 3 Ortep 3 view of the asymmetric unit (**1a**), Ellipsoids are drawn at the 30 % probability level, Hydrogen atoms are shows as spheres of arbitrary radii

Results and Discussion

Spectroscopic Analysis

The FTIR spectrum of (**1a**) gave a vibration at 3376 cm^{-1} which was the vibration of a free hydroxyl group, a band at 1734 cm^{-1} was also observed identified as that of an ester carbonyl CO group, and another band at 1625 cm^{-1} attributed to C=C bond. ^{1}H NMR of the product (**1a**) shows two non-equivalent vinyl protons appear in mean field, Ha appears as a doublet at 6.36 ppm, against Hb appear as a doublet in the range 5.78–5.79 ppm; The protons of CHOH also resonates mean field between 5.86 and 5.89 ppm; while the proton of the hydroxyl function appears as a double wide on 1.4 ppm; Aromatic protons resonate in the usual region with different multiplicities of a product to another; the methyl group of the ester function resonates as a singlet at 3.84 ppm. While the signals of the quinoline ring

Table 2 Crystal data and structure refinement for (**1a**) and (**2a**)

1a	**2a**
Crystal data	
$C_{16}H_{17}NO_4$	$C_{15}H_{14}ClNO_3$
$Mr = 287.31$	$Mr = 291.72$
Triclinic, *P*-1	Orthorhombic, *Pna21*
Hall symbol: -*P* 1	Hall symbol: *P 2c-2n*
$a = 7.9145(12)$ Å	$a = 7.7237(12)$ Å
$b = 9.1412(11)$ Å	$b = 20.254(3)$ Å
$c = 10.7286(16)$ Å	$c = 8.7164(12)$ Å
$\alpha = 94.760(11)°$	$V = 1363.6(3)$ A^3
$\beta = 105.988(13)°$	$Z = 4$
$\gamma = 101.818(11)°$	$F(000) = 608$
$V = 722.29(18)$ A^3	$Dx = 1.421$ Mg m^{-3}
$Z = 2$	Mo $K\alpha$ radiation, $\lambda = 0.71073$ Å
$F(000) = 304$	Cell parameters from 4254 reflections
$Dx = 1.321$ Mg m^{-3}	$\theta = 3.5–29.6°$
Mo $K\alpha$ radiation, $\lambda = 0.71073$ Å	$\mu = 0.29$ mm^{-1}
Cell parameters from 3524 reflections	$T = 150$ K
$\theta = 3.9–29.4°$	Block, colorless
$\mu = 0.10$ mm^{-1}	0.49 × 0.45 × 0.28 mm
$T = 150$ K	
Block, colorless	
0.32 × 0.27 × 0.13 mm	
Refinement	
Refinement on *F*2	Refinement on *F*2
Least-squares matrix: full	Least-squares matrix: full
$R[F2 > 2\sigma(F2)] = 0.070$	$R[F2 > 2\sigma(F2)] = 0.055$
$wR(F2) = 0.177$	$wR(F2) = 0.077$
$S = 1.108$	$S = 1.089$
3421 reflections	3296 reflections
220 parameters	187 parameters
0 restraints	1 restraint
Primary atom site location: structure-invariant direct methods	Primary atom site location: direct
Secondary atom site location: difference Fourier map	Hydrogen site location: difference Fourier map
Hydrogen site location: inferred from neighbouring sites	H atoms treated by a mixture of independent and constrained refinement
H atoms treated by a mixture of independent and constrained refinement	
$w = 1/[\sigma2(Fo2) + (0.1009P)2 + 0.3879P]$	$w = 1/[\sigma2(Fo\ 2) + (0.0437P)2 + 2.3066P]$
where $P = (Fo2 + 2Fc2)/3$	where $P = (Fo2 + 2Fc2)/3$
$(\Delta/\sigma)max = 0.009$	$(\Delta/\sigma)max = 0.0002$
$\Delta\rho max = 0.315$e A^{-3}	$\Delta\rho max = 0.447$ e A^{-3}
$\Delta\rho min = -0.281$ e A^{-3}	$\Delta\rho min = -0.66$ e A^{-3}
Extinction correction: *SHELXL*,	Extinction correction: *SHELXL*,
$Fc^* = kFc[1 + 0.001 \times Fc2\lambda3/\sin(2\theta)] -1/4$	$Fc^* = kFc[1 + 0.001xFc2\lambda3/\sin(2\theta)] - 1/4$
Extinction coefficient: 0.036 (9)	Extinction coefficient: 0.0509 (18)

substituents are either methyl groups which resonate as in a singlet 1.1 ppm or; the methoxyl groups appears as a singlet at 4.4 ppm.

The IR spectrum (**2a**) shows a band at 1714 cm^{-1} which was characterised as the carbonyl of the ester group vibrations, another vibrational band at 1602 cm^{-1}

attributed to C=C bond, and another peak at 774 cm^{-1} is assigned to the C–Cl stretching vibration. The ^1H NMR spectrum gave two singlet at 2.5 ppm and another slightly downfield 3.7 ppm integrating for three protons each attributed to the methoxy protons CO–O–CH_3 and O–CH_3 respectly, the singlet at 4.0 ppm is due to the two protons (CH_2–Cl) and the signal at 5.2 ppm may be attributed to the olefinic proton (C=CH).

Crystal Structure Analysis

The obtained compound (**1a**) (Fig. 3), crystallizes in P^{-1} space group with one molecule of methyl 2-[hydroxy(2-methoxy-8-methylquinolin-3-yl)methyl]prop-2-enoate in the asymmetric part of the unit cell. The molecular structure of (**1a**) derivative and the atom-labelling scheme are shown in (Fig. 3). The crystal and refinement data are given in (Table 2).

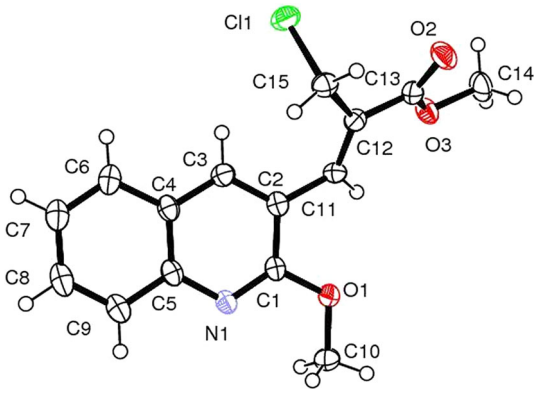

Fig. 4 Ortep 3 view of the asymmetric unit (**2a**), Ellipsoids are drawn at the 30 % probability level, Hydrogen atoms are shows as spheres of arbitrary radii

However the quinoline derivative (**2a**) (Fig. 4), crystallizes in non-centrosymmetric *Pna21* space group. Its asymmetric unit contains one methyl (2*Z*)-2-(chloromethyl)-3-(2-methoxyquinolin-3-yl)prop-2-enoate molecule. The molecular structure of the quinoline derivative (**2a**) and the atom-labelling scheme are shown in (Fig. 4). The crystal and refinement data are given in (Table 2).

The bonds distances within the quinoline portion of the molecules show evidence for significant bonds fixation; the N1–C1 bands (1.294(3) Å) **1a**; (1.310(5) Å) **2a** were significantly shorter than N1–C5 (1.375(3) Å) **1a**; (1.368(5) Å) **2a**, while the C2–C3 (1.363(3) Å) **1a**; (1.367(5) Å) **2a**, C6–C7 (1.371(4) Å) **1a**; (1.370(5) Å) **2a**, and C8–C9 (1.380 (4)Å) **1a**; (1.377(6) Å) **2a**, bands are all significantly shorter than the other aromatic C–C bonds. These distances compare well with the results observed in similar derivatives [2, 30, 31] selected bond lengths and angles of the structures are given in (Table 3).

The geometry withing the methyl 2-[hydroxy(2-methoxy-8-methylquinolin-3-yl)methyl]prop-2-enoate (**1a**) and methyl (2*Z*)-2-(chloromethyl)-3-(2-methoxyquinolin-3-yl)prop-2-enoate (**2a**) molecules are usual, the bonds distances and angles are in good agreement with those observed in similar compounds [32, 33].

The crystal packing (**1a**) is stabilized by variety of hydrogen bonding interactions O_2–H_2···O3, C6–H6···O2 (Fig. 5; Table 4). The intermolecular connection between

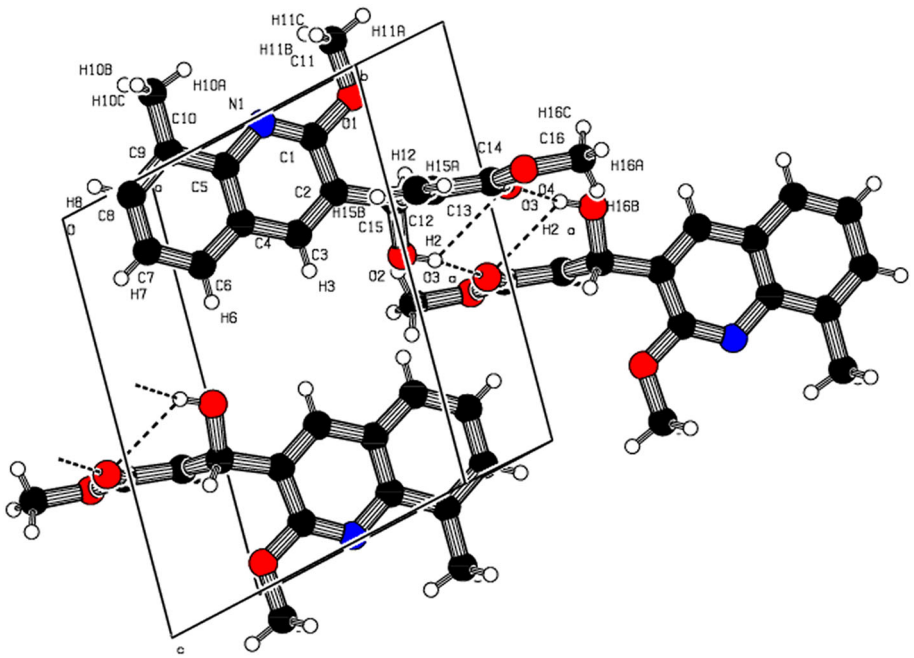

Fig. 5 Hydrogen bond interaction (**1a**) assuring the crystal structure cohesion

Table 3 Selected geometric parameters (Å, °) for (**1a**) and (**2a**)

1a				**2a**			
Bond distances							
O1–C1	1.355(2)	C3–C4	1.417(3)	Cl1–C15	1.819(4)	C3–C4	1.402(5)
O1–C11	1.433(3)	C4–C6	1.415(3)	O1–C1	1.355(4)	C4–C5	1.406(5)
O2–C12	1.425(2)	C4–C5	1.415(3)	O1–C10	1.428(4)	C4–C6	1.426(5)
O3–C14	1.215(3)	C5–C9	1.420(3)	O2–C13	1.217(5)	C5–C9	1.406(6)
O4–C14	1.329(3)	C6–C7	1.371(4)	O3–C13	1.335(4)	C6–C7	1.370(5)
O4–C16	1.437(3)	C7–C8	1.400(4)	O3–C14	1.447(5)	C7–C8	1.387(6)
N1–C1	1.294(3)	C8–C9	1.380(4)	N1–C1	1.310(5)	C8–C9	1.377(6)
N1–C5	1.375(3)	C9–C10	1.499(3)	N1–C5	1.368(5)	C11–C12	1.347(5)
C1–C2	1.432(3)	C12–C13	1.519(3)	C1–C2	1.421(5)	C12–C13	1.479(5)
C2–C12	1.506(3)	C13–C14	1.479(3)	C2–C3	1.367(5)	C12–C15	1.483(5)
C2–C3	1.363(3)	C13–C15	1.327(3)	C2–C11	1.462(5)		
Bond angles							
C1–O1–C11	116.33(18)	C4–C6–C7	119.3(2)	C1–O1–C10	116.3(3)	C4–C6–C7	120.0(4)
C14–O4–C16	116.0(2)	C6–C7–C8	120.8(2)	C13–O3–C14	115.6(3)	C6–C7–C8	120.0(4)
C1–N1–C5	117.55(17)	C7–C8–C9	122.1(2)	C1–N1–C5	117.6(3)	C7–C8–C9	121.8(4)
O1–C1–C2	114.11(17)	C5–C9–C8	117.73(19)	O1–C1–N1	119.5(3)	C5–C9–C8	119.4(4)
N1–C1–C2	125.82(18)	C5–C9–C10	119.7(2)	O1–C1–C2	115.1(3)	C2–C11–C12	126.6(3)
O1–C1–N1	120.07(17)	C8–C9–C10	122.6(2)	N1–C1–C2	125.4(3)	C11–C12–C13	120.4(3)
C1–C2–C12	119.69(17)	O2–C12–C2	108.83(15)	C1–C2–C3	116.0(3)	C11–C12–C15	125.3(3)
C3–C2–C12	123.75(17)	O2–C12–C13	110.29(16)	C1–C2–C11	119.6(3)	C13–C12–C15	114.3(3)
C1–C2–C3	116.55(18)	C2–C12–C13	112.91(19)	C3–C2–C11	124.4(3)	O2–C13–O3	122.7(3)
C2–C3–C4	120.34(18)	C12–C13–C15	124.77(18)	C2–C3–C4	121.3(3)	O2–C13–C12	123.2(3)
C3–C4–C6	122.49(19)	C14–C13–C15	121.52(18)	C3–C4–C5	117.7(3)	O3–C13–C12	114.1(3)
C5–C4–C6	119.60(19)	C12–C13–C14	113.7(2)	C3–C4–C6	123.1(3)	Cl1–C15–C12	109.3(3)
C3–C4–C5	117.91(18)	O3–C14–C13	122.74(19)	C5–C4–C6	119.2(3)		
N1–C5–C9	117.69(18)	O4–C14–C13	114.3(2)	N1–C5–C4	121.9(3)		
C4–C5–C9	120.50(18)	O3–C14–O4	122.91(19)	N1–C5–C9	118.5(3)		
N1–C5–C4	121.81(18)			C4–C5–C9	119.6(3)		
Torsion angles							
C4–C6–C7–C8	0.5(4)	C16–O4–C14–O3	1.3(3)	C10–O1–C1–N1	4.7(4)	C4–C6–C7–C8	0.0(6)
C4–C5–C9–C8	0.9(4)	C16–O4–C14–C13	−177.7(1)	C10–O1–C1–C2	−175.9(3)	C3–C4–C5–C9	178.1(4)
N1–C5–C9–C8	−179.1(2)	N1–C1–C2–C12	177.9(2)	C3–C4–C5–N1	−1.3(6)	C6–C4–C5–N1	178.6(3)
C5–N1–C1–O1	−179.6(2)	C12–C2–C3–C4	−178.8(2)	C6–C4–C5–C9	−1.9(6)	N1–C1–C2–C11	−178.3(3)
C5–N1–C1–C2	0.9(3)	C1–C2–C12–O2	−161.6(2)	C5–N1–C1–O1	179.5(3)	C3–C4–C6–C7	−178.5(4)
C1–N1–C5–C9	−179.9(2)	C3–C2–C12–O2	17.2(3)	C5–N1–C1–C2	0.1(5)	C3–C2–C11–C12	38.2(6)
O1–C1–C2–C3	179.5(2)	O1–C1–C2–C12	−1.6(3)	C1–N1–C5–C4	1.9(5)	N1–C5–C9–C8	−179.8(4)
C6–C4–C5–N1	179.0(2)	N1–C5–C9–C10	0.4(3)	C1–N1–C5–C9	−177.6(3)	C1–C2–C11–C12	−146.4(4)
N1–C1–C2–C3	−1.0(4)	C11–O1–C1–C2	179.5(2)	O1–C1–C2–C3	178.1(3)	C14–O3–C13–O2	1.7(5)
C3–C4–C5–C9	179.1(2)	C4–C5–C9–C10	−179.6(2)	O1–C1–C2–C11	2.3(4)	C14–O3–C13–C12	−179.2(3)
C6–C4–C5–C9	−1.0(4)	C7–C8–C9–C10	−179.7(2)	N1–C1–C2–C3	−2.6(5)		
C3–C4–C6–C7	−179.8(2)	O2–C12–C13–C14	75.6(2)	C6–C7–C8–C9	−1.2(6)		
C5–C4–C6–C7	0.3(4)	C2–C12–C13–C1	−162.4(1)	C1–C2–C3–C4	3.1(5)		
C2–C3–C4–C5	0.8(3)	C2–C12–C13–C15	19.1(3)	C11–C2–C3–C4	178.6(3)		
C2–C3–C4–C6	−179.1(2)	C12–C13–C14–O3	−3.3(3)	C5–C4–C6–C7	1.5(6)		
C3–C4–C5–N1	−0.9(3)	C15–C13–C14–O3	175.2(2)	C4–C5–C9–C8	0.7(6)		
C6–C7–C8–C9	−0.5(4)	C1–C2–C12–C13	75.6(3)	C2–C3–C4–C5	−1.3(6)		
C7–C8–C9–C5	−0.2(4)	C16–O4–C14–O3	1.3(3)	C2–C3–C4–C6	178.7(4)		

Table 4 Hydrogen bond geometry (Å, °) of the (**1a**) quinoline derivative; Symmetry codes: (i) 2 − x, 2 − y, 1 − z; (ii) 1 − x, 1 − y,1 − z

D–H···A	D–H	H···A	D···A	D–H···A
O2–H2···O3	0.88(3)	2.58(3)	3.067(2)	115.5(19)
O2–H2···O3^{i}	0.88(3)	2.01(2)	2.860(2)	161(2)
C6–H6···O2^{ii}	0.99(2)	2.41(2)	3.366(3)	163(2)

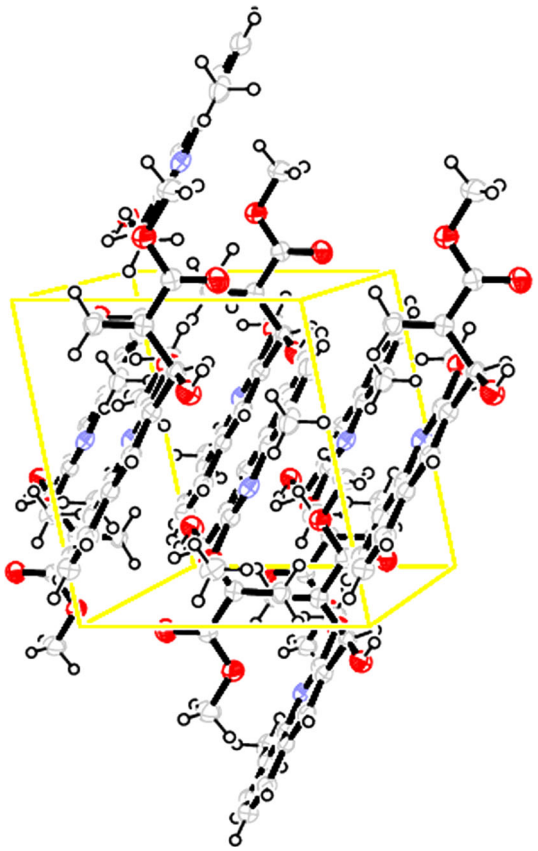

Fig. 6 Ortep 3 projection of the (**1a**) crystal structure on the (001) direction

Table 5 Hydrogen bond geometry (Å, °) of the (**2a**) quinoline derivative; Symmetry codes: (i) 1/2 − x,−1/2 + y,−1/2 + z

D–H···A	D–H	H···A	D···A	D–H···A
C9–H9···O2^{i}	0.96(4)	2.52(4)	3.418(5)	156(3)

methyl 2-[hydroxy(2-methoxy-8-methylquinolin-3-yl)methyl]prop-2-enoate (**1a**) molecules develops According to C axis (Fig. 6).

However the crystal packing (**2a**) is stabilized by a hydrogen bonding interaction C9–H9···O2 (Fig. 7; Table 5), The intermolecular connection between methyl (2*Z*)-2-(chloromethyl)-3-(2-methoxyquinolin-3-yl) prop-2-enoate (**2a**) molecules is stabilized by Intramolecular hydrogen bonds (Table 5). In the crystal structure, the molecules are stacked in layers (Fig. 8).

In the packings of **1a** and **2a**, π-type interactions seem to play an important role, but the π···π interactions were precluded by the methyl and methoxy groups,

Biological Activity

The aim of the synthesis of any antimicrobial compound is to inhibit the causal microbe without any secondary effects on the patients. In addition, it is worthy to stress here on the basic idea of applying any chemotherapeutic agent which depends essentially on the specific control of only one biological function and not multiple ones [34].

In testing the antibacterial activity of these compounds (Table 6) we used more than one test organism to increase the chance of detecting antibiotic principles in the tested materials. The sensitivity of a microorganism to antibiotics and other antimicrobial agents was determined by the assay plates which incubated at 37 °C for 1 day for bacteria.

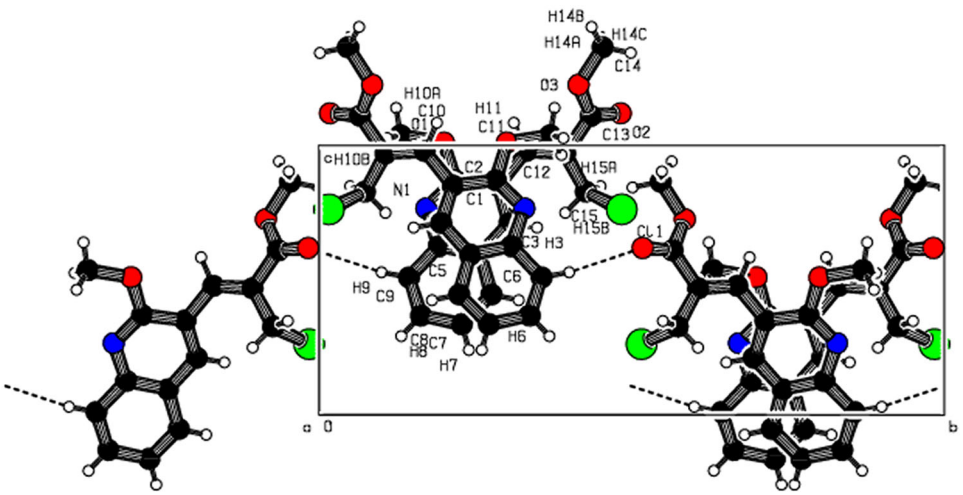

Fig. 7 Platon (XO) view visualising the hydrogen bonds in (**2a**)

Both of the tested compounds showed a remarkable biological activity against different types of Gram-positive (*S. aurous; Staphylococcus* coagulase-negative), Gram-negative (*E. coli*; *P. aeruginosa*) bacteria. The data obtained are listed in Table 6. On comparing the biological activity of the quinoline compounds with the standard Oflaxacine (OFX) and Ciprofloxacine (CIP) (antibacterial agent), it is seen that:

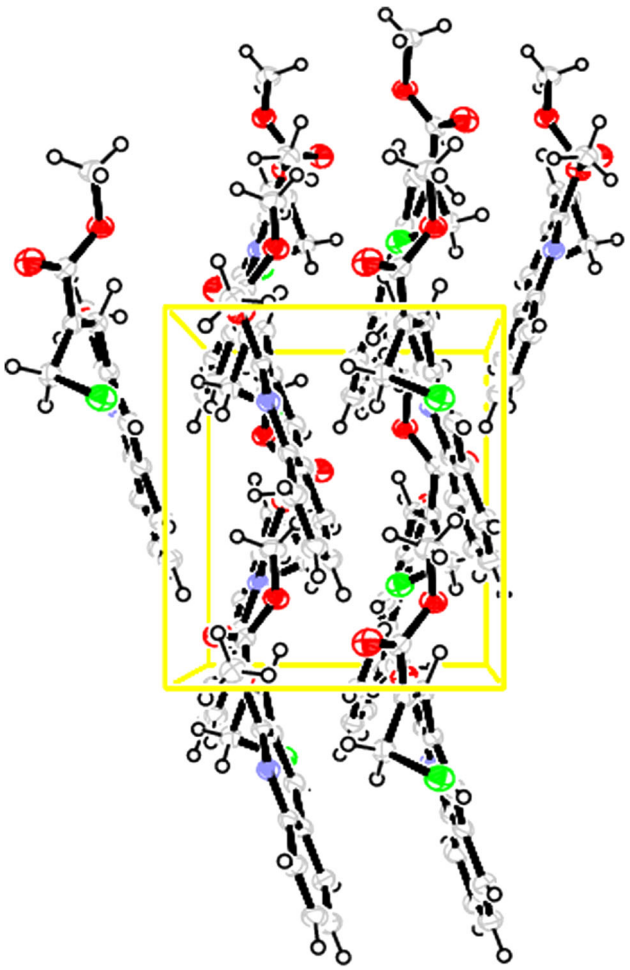

Fig. 8 Ortep 3projection of the (**2a**) crystal on the (010) direction

(1) The biological activity with Gram-positive bacteria of quinoline is good in comparison with the standards used.
(2) Compounds (**1a**) showed maximum activity for maximum concentration [4 mg/ml] (20 mm) zone size against *S. aurous* and (18 mm) zone size against *Staphylococcus* coagulase-negative activity. While Compounds (**2a**) showed maximum activity with also maximum concentration [4 mg/ml] (22 mm) zone size *S. aurous* and (22 mm) zone size against *Staphylococcus* coagulase-negative activity.
(3) It has no biological activity towards Gram-negative bacteria (*E. coli* and *P. aeruginosa*).

Conclusion

In summary, two new Quinoline derivatives have been prepared; between Baylis–Hillman products which had themselves been prepared from the Meth Cohn method; catalyzed by 1,4-diazabicyclo [2] octane (DABCO) and silicium oxid or in pyridine and chloroform.

The good products yields, the, simple starting materials, and the mild reaction conditions are the main advantages of this reactions.

Chemical structures have been determinate by spectral techniques of FTIR, ^{1}H NMR, and X-ray single crystal in low temperature. The moving of IR and NMR spectra description were obtains before the crystal structure description; which proves that we obtain extremely pure products.

This new Quinoline derivatives constitute an original compounds, of great interest biological activity.

Supplementary Material

CCDC 1044714 and 1044715 contains the supplementary crystallographic data for this paper. These data can be obtained free of charge via http://www.ccdc.cam.ac.uk/

Table 6 Biological activity of **1a**, **2a**

Compound	Inhibition zone diameter (mm/mg sample)									
	Gram+								Gram−	
	Staphylococcus aurous				*Staphylococcus* coagulase-negative				*Escherichia coli*	*Pseudomonas aeruginosa*
mg/ml	4	3	2	1	4	3	2	1	4–1	4–1
(**1a**)	20	19	18	16	18	17	15	14	<6	<6
(**2a**)	21	20	17	14	22	20	19	16	<6	<6
OFX	26				30				32	19
CIP	29				32				37	33

conts/retrieving.html (or from the Cambridge Crystallographic Data Centre, 12, Union Road, Cambridge CB2 1EZ, UK; fax: 00441223 336033.

Acknowledgments The authors acknowledge The Tassili Programme N° 15MDU940 for the financial support. In addition, A.M and T.D acknowledge the help and advice of M.R.Y.El-Hillou (Université Larbi Ben Mhidi Oum El Bouaghi).

References

1. Michael JP (1997) Nat Prod Rep 14:605
2. Fatiha G, Amani D, Mohammed L, Nourredine B (2012) J Chem Crystallogr 42:989–996
3. Levy S, Azoulay SJ (1994) Cardiovas Electrophysiol 5:635–636
4. Wenckebach KF (1923) JAMA 81:472–474
5. Roma G, Braccio MD, Grossi G, Mattioli F, Ghia H (2000) Eur J Med Chem 35:1021–1035
6. Bilker O, Lindo V, Panico M, Etiene AE, Paxton T, Dell A, Rogers M, Sinden RE, Morris HR (1998) Nature 392:289–292
7. Vargas LY, Castelli MV, Kouznetsov VV, Urbina JM, Lopez SN, Sortino M, Enriz RD, Ribas JC, Zacchino S (2003) Bioorg Med Chem 11:1531–1550
8. Phan LT, Jian T, Chen Z, Qiu Y-L, Wang Z, Beach T, Polemeropoulos A, Or YS (2004) J Med Chem 47:2965–2968
9. Fang K-C, Chen Y-L, Sheu J-Y, Wang T-C, Tzeng C-C (2000) J Med Chem 43:3809–3812
10. Bailly C, Laine W, Baldeyrou B, De Pauw-Gillet M-C, Colson P, Houssier C, Cimanga K, Miert SV, Vlietinck AJ, Pieters L (2000) Anti-Cancer Drug Des 15:191–201
11. Dassonneville L, Bonjean K, De Pauw-Gillet M-C, Colson P, Houssier C, Quetin-Leclercq J, Angenot L, Ablordeppey SY (2002) Bioorg Med Chem 10:1337–1346
12. Khan MTH (2007) Quinoline analogs as antiangiogenic agents and telomerase inhibitors. In: Khan MTH, Gupta R (eds) Bioactive heterocycles V.R. Springer, Berlin **Top Heterocycl Chem 11:213–229**
13. Cheng X-M, Lee C, Klutchko S, Winters T, Reynolds EE, Welch KM, Flynn MA, Doherty AM (1996) Bioorg Med Chem 6:2999
14. Anzini M, Cappelli A, Vomero S, Giorgi G, Langer T, Hamon M, Merahi N, Emerit BM, Cagnotto A, Skorupska M, Mennini T, Pinto JC (1995) J Med Chem 38:2692
15. Giardina GAM, Sarau HM, Farina C, Medhurst AD, Grugni M, Raveglia LF, Schmidt DB, Rigolio R, Luttmann M, Vecchietti V, Hay DWP (1997) J Med Chem 50:1794
16. Holla BS, Mahalinga M, Karthikeyan MS, Akberalib PM, Shettyc NS (2006) Bioorg Med Chem 14:2040–2047
17. Całus S, Gondek E, Danel A, Jarosz B, Pokładko M, Kityk AV (2007) Mater Lett 61:3292–3295
18. Baylis AB, Hillman MED (1972) German patent, 21155113. Chem Abstr 77:34174
19. Meth Cohn O, Narine B, Tarnowski B (1981) J Chem Soc Perkin Trans 1:1520–1530
20. Narender P, Srinivas U, Gangadasu B, Biswas S, Jayathirtha Rao V (2005) Bioorg Med Chem Lett 15:5378–5381
21. Oxford Diffraction (2006) Xcalibur CCD system, CrysAlis Software system, Version 1.171. Oxford Diffraction Ltd., Abington
22. Farrugia LJ (1999) J Appl Crystallogr 32:837–838
23. Burla MC, Caliandro R, Camalli M, Carrozzini B, Cascarano GL, De Caro L, Giacovazzo C, Polidori G, Spagna R (2005) J Appl Crystallogr 38:381–388
24. Sheldrick GM (1997) SHELXL97. University of Göttingen, Germany
25. Farrugia LJ (1997) J Appl Crystallogr 30:565
26. Bruno IJ, Cole JC, Edgington PR, Kessler M, Macrae CF, McCabe P, Pearson J, Taylor R (2002) Acta Cryst B58:389–397
27. Spek AL (2003) J Appl Crystallogr 36:7–13
28. Grayer RJ, Harbone JB (1994) Photochemistry 73:19
29. Irob ON, Moo-Young M, Anderson WA (1996) Int J Pharmacol 34:87
30. Kalkhambkar RG, Kulkarni GM, Hwang WS, Lee CS (2008) Acta Cryst E 64:o258
31. Benzerka S, Bouraiou A, Bouacida S, Debache A, Belfaitah A (2008) Acta Cryst E 64:o2115–o2116
32. Insuasty B, Torres H, Cobo J, Lowd JN, Gilidewell C (2006) Acta Cryst C 62:O39–O41
33. Jasinski JP, Bucher RJ, Mayekar AN, Yathirajan HS, Narayama B, Sarojini BK (2010) J Mol Struc 980:172–181
34. Sayed MA, Zayed MA, Gehad GM (2010) Arab. J. Chem 3:103–113